Check for updates

# Surface-enhanced Raman spectroscopy of microorganisms: limitations and applicability on the single-cell level†

Ruben Weiss, [a] Márton Palatinszky, [b] Michael Wagner, [b] Reinhard Niessner, [a] Martin Elsner, [a] Michael Seidel [a] and Natalia P. Ivleva *[a]

Detection and characterization of microorganisms is essential for both clinical diagnostics and environmental studies. An emerging technique to analyse microbes at single-cell resolution is surface-enhanced Raman spectroscopy (surface-enhanced Raman scattering: SERS). Optimised SERS procedures enable fast analytical read-outs with specific molecular information, providing insight into the chemical composition of microbiological samples. Knowledge about the origin of microbial SERS signals and parameter(s) affecting their occurrence, intensity and/or reproducibility is crucial for reliable SERS-based analyses. In this work, we explore the feasibility and limitations of the SERS approach for characterizing microbial cells and investigate the applicability of SERS for single-cell sorting as well as for three-dimensional visualization of microbial communities. Analyses of six different microbial species (an archaeon, two Gram-positive bacteria, three Gram-negative bacteria) showed that for several of these organisms distinct features in their SERS spectra were lacking. As additional confounding factor, the physiological conditions of the cells (as influenced by *e.g.*, storage conditions or deuterium-labelling) were systematically addressed, for which we conclude that the respective SERS signal at the single-cell level is strongly influenced by the metabolic activity of the analysed cells. While this finding complicates the interpretation of SERS data, it may on the other hand enable probing of the metabolic state of individual cells within microbial populations of interest.

## Introduction

In the last decade surface-enhanced Raman scattering (SERS) has received increasing attention for the analysis of biological samples, ranging from environmental studies[1–4] to diagnostics.[5–8] The underlying principle of Raman spectroscopy (RS) is based on the inelastic scattering of light giving rise to characteristic spectra that yield chemical information in a non-invasive, non-destructive way with little interference of water. Combining the band-related data of the spectrometer with the spatial information of a confocal microscope, enables analyses of sample material with a spatial resolution in the micrometre-range necessary for studying the chemical composition of microbes on a single-cell level. The resolution is physically limited by the diffraction defined through the excitation wavelength and numerical aperture of the microscope objective. Thus, with RS the analysis of single microbial cells under natural conditions is possible. If combined with stable isotope probing, the activity of microbial cells within their habitat can be deduced from red-shifts of certain peaks in the spectra of active cells[9,10] and if desired such analyses can be combined with identification of the respective organisms with fluorescence *in situ* hybridization (FISH).[11] Excitingly, recent technological developments even allow sorting of individual microbial cells with selected characteristics within their Raman spectra for subsequent genomic analysis or cultivation.[12]

Sorting of single cells by means of optical trapping and discrimination by RS (laser tweezer Raman spectroscopy: LTRS or Raman tweezers) was introduced by Xie, Chen and Li[13] and applied in several studies. Huang *et al.* showed that single cells of unlabelled *Escherichia coli* and ^{13}C-labelled *Pseudomonas fluorescens* from a mixed population can be isolated by Raman tweezers.[14] A recent study by Berry *et al.* used LTRS to detect incorporation of deuterium into cecal micro-

*[a]Technical University of Munich, Institute of Hydrochemistry, Chair of Analytical Chemistry and Water Chemistry, Marchioninistrasse 17, D-81377 Munich, Germany. E-mail: natalia.ivleva@ch.tum.de; Fax: +49 89 2180 78255; Tel: +49 89 2180 78252*
*[b]University of Vienna, Department of Microbiology and Ecosystem Science, Division of Microbial Ecology, Research Network "Chemistry meets Microbiology", Althanstrasse 14, A-1090 Vienna, Austria*
†Electronic supplementary information (ESI) available: Additional information as mentioned in the text. See DOI: 10.1039/c8an02177e

biota of mice as a marker for metabolic activity.[9] Subsequently, genomic information of sorted microbial cells was analysed by whole genome amplification and sequencing. Wang *et al.* introduced another method for the sorting of single cells by RS in combination with laser-induced forward transfer and termed the technique Raman activated cell ejection (RACE).[15]

In conventional RS, the analytical throughput is limited because of the low scattering cross section. SERS offers an improvement with enhancement factors of up to $10^{11}$.[16] The underlying principle is that surfaces of nanosized metal structures (Ag or Au) can enhance the local electric field of the excitation source because of surface plasmon resonance. Scattering intensities increase since the Raman effect depends on the electric field strength. Also, the polarizability of molecules directly attached to these metal surfaces changes, enhancing the resultant Raman scattering.

In 1998 Efrima and Bronk showed the general applicability of SERS for the analysis of bacteria.[17] Species- and even strain-specific characterization was demonstrated by Jarvis and Goodacre in 2004.[18] In 2007 Kahraman *et al.* illustrated that the SERS analysis down to a few bacterial cells can be realised.[19] Kubryk *et al.* presented 2015 a reproducible SERS analysis of bacteria at the single-cell level with the capability of detecting stable isotope incorporation.[20] The characteristics of microbial SERS spectra were mainly attributed to flavins[21] and peptidoglycan.[18] Recently, major contributions of adenine-derived compounds were recognised with a marker band at about 730 cm$^{-1}$.[22,23] Controversially, Chisanga *et al.* applying a different sample preparation protocol observed the absence of this prominent SERS peak.[24] Premasiri *et al.* reported that SERS spectra of bacteria display the salvaging pathways and secretion of purines.[23] Molecules, which contribute to the SERS signal and only occur intracellular or are anchored to the cell envelope, are not complicating the analyses. In contrast, extracellular released compounds detected by SERS render the assignment of a SERS signal to defined cells very challenging. Degradation pathways, secretion/excretion processes and shock reactions heavily depend on the physiological state of the microorganisms and might also be influenced by the sample preparation. Therefore, studies are needed to clarify the mechanism causing SERS signals of microbial samples and to address the factors that influence the composition of resulting spectra which might – in the worst case – lead to erroneous results. In 2015 Zhou *et al.* reported that the differentiation of live and dead bacteria is possible by SERS because of disappearing signals for dead cells.[25] In the present study, we confirm this observation but critically evaluate whether the missing peaks may be used as an indicator for dead bacteria or rather as evidence for metabolic inactivity.

In the first part of this work, SERS signals from six phylogenetically diverse microorganisms representing different cell envelope types including an archaeon and Gram-positive as well as Gram-negative bacteria were analysed to investigate the variability and reproducibility of SERS for the analyses of microbes. In addition, to outline potential limitations, the Gram-negative model bacterium *Escherichia coli* was chosen to study the effect of varying physiological conditions such as storage times and growth in heavy water on the SERS signal. Finally, in the second section of this study, the applicability of SERS for LTRS of microbial cells and for three-dimensional analyses of biological samples was evaluated.

# Experimental

## Chemicals and materials

Standard chemicals were purchased from Carl Roth GmbH & Co. KG (Karlsruhe, Germany), Merck KGaA (Darmstadt, Germany) or Sigma-Aldrich (Vienna, Austria; Steinheim, Germany). $^{13}C_6$-D-glucose ($^{13}C_6H_{12}O_6$) and $D_2O$ were obtained from Sigma-Aldrich. The Colilert-18 test kit was purchased from IDEXX Europe B.V. (Hoofddorp, Netherlands) and the LIVE/DEAD *Bac*Light kit from Life Technologies GmbH (Darmstadt, Germany). Only purified water was used (Milli-Q, Merck KGaA). Glass capillaries with internal dimensions of 100 μm × 1 mm × 50 mm and a wall thickness of 70 μm were purchased from CM Scientific (Silsden, United Kingdom).

## Microorganisms

Bacterial strains were either obtained from the German Collection of Microorganisms and Cell Cultures (DSMZ, Braunschweig, Germany) or LGC Standards GmbH (Wesel, Germany). *Bacillus subtilis* (DSM 1087), *Escherichia coli* (DSM 498; DSM 1116), *Micrococcus luteus* (DSM 20030) and *Pseudomonas putida* (ATCC 12633) were cultured aerobically with LB and a supplemented M9 minimal medium as biological triplicates to the stationary phase (see ESI Fig. S1a†). *Nitrospira inopinata* (DSM 105286)[26] and *Nitrososphaera gargensis* (DSM 103042)[27,28] were obtained from culture collection of the Division of Microbial Ecology at the University Vienna but are also available from the DSMZ. These strains were cultured in a mineral salt medium with ammonium as energy source as described previously.[28] Detailed procedures on the cultivation are included in the ESI.†

## *In situ* sample preparation for SERS analysis

The silver colloid synthesis applied in this study is based on the method by Leopold and Lendl.[29] It was performed *in situ*[30] and followed the modified procedure as described elsewhere.[20] Microbial cultures were either used directly or stored at 5 °C up to 5 days before silver nanoparticle (AgNP) synthesis. As this synthesis was performed equally 1 h prior to SERS measurements we disregarded the reported disadvantageous behaviour of toxic silver[31] for the SERS analysis of bacteria. It is irrelevant for the findings of our study if the analysed microorganisms are killed during the *in situ* AgNP synthesis. Surprisingly, cultivation experiments with treated *E. coli* cells show still microbial growth (comp. ESI Fig. S1a†). Although *E. coli* strain W is non-mucoid it is known to form capsular polysaccharides at temperatures below 15 °C.[32] Therefore, microbial cells were washed before nanoparticle synthesis to

avoid interferences with the colloid synthesis. For this purpose, 1 ml of the culture was centrifuged (5500$g$, 1 min, 20 °C), the supernatant discarded and the cell pellet resuspended with water. This washing step was repeated twice. After the third centrifugation, the cell pellet was resuspended with 450 μl of a reducing solution. For SERS analysis with a 633 nm laser the reducing solution was prepared by dissolving 11.6 mg $NH_2OH \cdot HCl$ in 96.7 ml water and adding 3.3 ml of a 0.1 M sodium hydroxide solution. Finally, 50 μl a 10 mM silver nitrate solution was added to the resuspended microbial cells at room temperature to form AgNP on the cell surface. For SERS analysis with an excitation wavelength of 532 nm the concentration of all reagents was doubled and colloidal *in situ* synthesis was performed at 5 °C. The reagents were mixed by inverting the sample three times. The sample colour changed instantly to yellowish-grey indicating the formation of silver nanoparticles (comp. ESI Fig. S2†). For dried samples, 1 μl of the cell suspension was spotted onto a glass slide after a reaction time of 1 h if not stated otherwise. The spot was dried at room temperature for at least 30 min. For the artificial biofilm, a 2% (m/m) suspension of agarose was stirred under reflux at 90 °C for 5 min. Subsequently, at 37 °C 300 μl of each $^{12}C$- and $^{13}C$-labelled colloidal sample were added to 8.4 ml of the dissolved agarose, gently pivoted and casted (2 ml) into a preheated Petri dish with a diameter of 5 cm. The resulting gels were covered with water. For the tweezing experiments with a mixture of $^{12}C/^{13}C$-labelled cells 0.5 μl of each separately prepared sample was used. In accordance to Berry *et al.*[9] a small volume of this suspension was drawn into rectangular glass capillaries which was already filled to about three quarters with a phosphate-buffered saline (PBS) with 5.6 mg $L^{-1}$ Tween 20. Particles could be moved through this interface between the two compartments to the cell-free region of the PBS buffer with the activated tweezer laser by moving the capillary with the motorised microscope stage. The inlets of the capillary were sealed with petrolatum.

### Raman microscopic analysis

All SERS analyses were performed with an LabRAM HR800 microspectrometer (Horiba Jobin Yvon, France) equipped with a frequency-doubled Nd:YAG laser (532 nm, 35 mW at the sample), a He–Ne laser (633 nm, 13.8 mW at the sample), a standard Nd:YAG laser for optical trapping (1064 nm, 500 mW at the sample), corresponding edge filters, a confocal pinhole set to a diameter of 100 μm, diffraction gratings with 300 or 600 lines per mm and a motorized microscope stage. The stage could be moved while optically trapping cells to sort them. The system was calibrated onto the first-order phonon band of silicon at 520.7 $cm^{-1}$. Dried samples were measured with a 100× objective (Olympus MPlan N, NA = 0.9). The laser beam was focused onto single cells with an acquisition time of 3 × 1 s and an intensity of 0.1% or 1% of the full laser power. A typical microscopic image of this kind of sample without and with laser illumination (see ESI Fig. S3a/b†) shows experimental evidence for the analysis at the single-cell level by SERS. The SERS spectra of different microorganisms presented in Fig. 1 and the spectra obtained from the optical tweezing setup were measured with the 532 nm laser and the grating with 300 lines per mm in one measurement window resulting in a spectral range of 400–3300 $cm^{-1}$. The optical trapping measurements were performed with a 63× water immersion objective (Zeiss
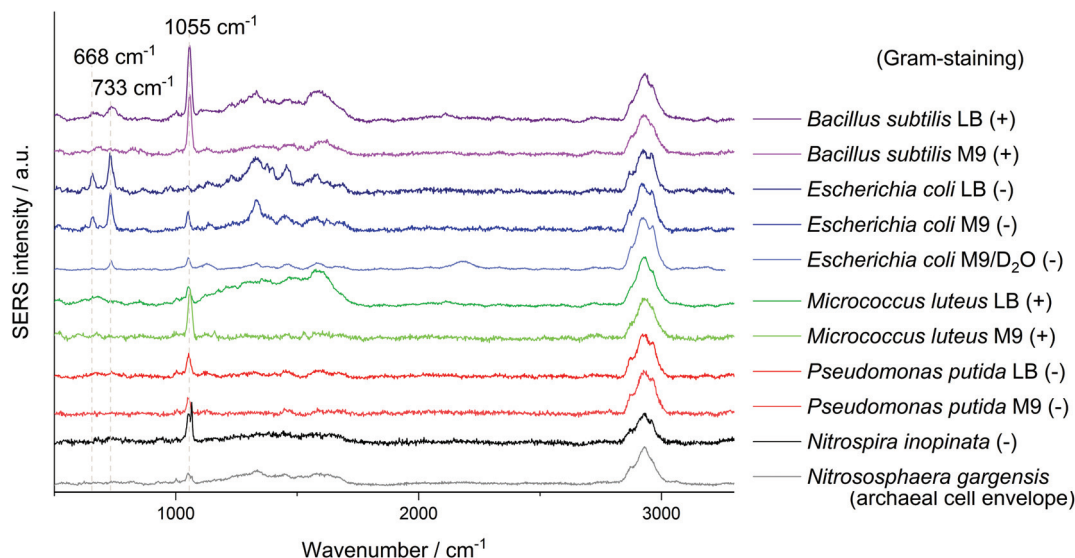


**Fig. 1** SERS mean spectra of at least 8 single cells of *B. subtilis*, *E. coli*, *M. luteus*, *P. putida*, *N. gargensis* and *N. inopinata* measured with an excitation wavelength of 532 nm. Spectra are baseline-corrected and normalised to the C–H stretching vibration, (+) and (−) indicate Gram-positive and -negative, respectively. M9 and LB refer to the different media used for cultivation of the respective species. $D_2O$ indicates that the organism was cultured with heavy water in the medium. The signal at 1084 $cm^{-1}$ for the complete nitrifier *N. inopinata* most probably results from precipitated $CaCO_3$ of the medium.

C-APOCHROMAT, NA = 1.2), 100 ms acquisition time, full power of the tweezing laser (500 mW) and reduced power of the excitation laser (3 mW). All other SERS spectra were acquired with an excitation wavelength of 633 nm and the grating with 600 lines per mm. The artificial biofilm was measured with a 60× water immersion objective (Olympus LUMPlanFL N, NA = 1.0), measurement time of 2 × 100 ms, laser intensity of 1.38 mW and static spectral region of 50–1260 cm$^{-1}$ and a spatial measurement interval of 1 μm. All spectra related to the storage series of E. coli (DSM 1116) were measured under equal conditions with the 633 nm laser, an effective laser power of 138 μW and five consecutive measurement windows resulting in the spectral range of 50–4000 cm$^{-1}$. In this measurement series 10 spectra of randomly chosen cells were acquired for each group of biological triplicates, respectively 30 spectra for the biological triplicates cultured with LB medium and a storage time of zero or four days. The evaluation of the non-normalised data from this series was performed automatically by MATLAB R2016a (The MathWorks, USA) in the spectral region of 700–760 cm$^{-1}$ by fitting a Lorentzian with a linear background. The signal intensity of the SERS peak at 733 cm$^{-1}$ was determined as the amplitude of the Lorentzian and is in all graphs simply referred to as SERS signal. The SERS spectra are marked as positive hits if the amplitude is bigger than three times the noise averaged over all spectra of one data point plus the baseline at the fitted peak (see ESI Fig. S3c†). The noise was calculated in the Raman silent region at 2500–2600 cm$^{-1}$. Spectra in Fig. 1 were baseline-corrected with a linear assumption and normalised to maximal intensity between 2900–2960 cm$^{-1}$ with LabSpec 6 (Horiba Jobin Yvon, France).

### Scanning electron microscopy

Samples were prepared in the same way as for the SERS preparation. The suspension was spotted directly onto the aluminium sample holder and dried at room temperature. A Sigma 300 VP scanning electron microscope (Carl Zeiss AG, Germany) was used. Images were recorded with the In-Lens detector, an acceleration voltage of up to 10 kV and a working distance between 2.8–3.1 mm.

## Results and discussion

### Limitations of SERS for microbial detection

**Spectral features and artefacts for SERS of microbial samples.** In the last decade numerous studies have reported SERS applications for the detection, characterization and identification of microorganisms because of the improved sensitivity of SERS compared to conventional RS.[33–36] Here in situ AgNP synthesis[20,30] was performed to facilitate SERS analysis of an array of different microorganisms with different types of cell envelopes: two Gram-positive bacteria, three Gram-negative bacteria and an archaeon. The normalised mean spectra with equal acquisition parameters at an excitation wavelength of 532 nm are depicted in Fig. 1. SERS spectra of all bacterial strains analysed showed characteristic C–H stretching vibrations at around 2930 cm$^{-1}$. An additional broad band at 2200 cm$^{-1}$ was observed in case of deuterium-labelled E. coli that can be attributed to the partial substitution of protium with deuterium which causes a red-shift of the C–D stretching compared to the C–H mode as explained by Berry et al. for discrimination by conventional RS.[9] As expected, this shift is also detectable in the conventional Raman spectra of single E. coli cells (see Fig. S4†). Contrastingly, the ratio of most SERS signals in the fingerprint region below 1500 cm$^{-1}$ to the C–H stretching vibration at 2930 cm$^{-1}$ is significantly smaller in comparison to the undeuterated sample of E. coli. A higher ratio could have been explained well by the aforementioned incorporation of deuterium and the resulting signal splitting. This reduction of signal intensities suggests that the growth of E. coli in the presence of heavy water affects its physiology in a way that also influences the process which lies at the heart of SERS.

Another signal shared by the spectra of several microorganisms lies at about 1055 cm$^{-1}$ which was so far mostly attributed to amine but also to phosphate (FAD),[24] carbohydrate[37] and nitrate[38] interacting with AgNP. Simple mixing experiments of AgNO$_3$ with NaNO$_3$ indicate that the Raman peaks of these nitrates at 1044 cm$^{-1}$ and 1067 cm$^{-1}$ combine to a broader band in between. The relatively high sodium concentration from the added sodium hydroxide for in situ nanoparticle synthesis might explain the position of the nitrate peak in SERS spectra with AgNO$_3$ as precursor. The reference spectra of other nitrates such as KNO$_3$ or Ca(NO$_3$)$_2$ show an intense signal at exactly 1050 cm$^{-1}$. As this band mainly occurs when AgNP were synthesised with hydroxylamine as reducing agent it might be related to an excess of hydroxylamine binding to the AgNP. Nitrate from the precursor AgNO$_3$ thermodynamically tends to comproportionate with hydroxylamine, diminishing the band at 1055 cm$^{-1}$ over time. As the AgNP synthesis is performed in a complex sample, trace elements might catalyse the decomposition of the reducing agent. Still it is surprising that for E. coli, especially if cultured in LB medium, the presumably unspecific peak at 1055 cm$^{-1}$ is significantly weaker. This could be related to the appearance of new peaks and a competitive binding of analytes with a higher affinity for AgNP.

The intense SERS signals observed for E. coli at 733 cm$^{-1}$ and 668 cm$^{-1}$ show the greatest variation in intensity between the investigated microorganisms (Fig. 1). In 2016 Kubryk et al.[22] and Premasiri et al.[23] assigned these bands to purine bases and biochemically relevant derivatives, e.g., adenine, guanine, hypoxanthine, xanthine, where Premasiri et al. found a perfect alignment of bacterial SERS spectra and these compounds. Earlier the frequently arising SERS peak at 733 cm$^{-1}$ had also been attributed to N-acetyl-D-glucosamine,[18] methylene rocking vibrations,[39] a glycosidic ring[18] and pyrophosphate mode[40] and was also thought to be loosely related to amino acids and phospholipids.[41] Surprisingly, a recent study by Chisanga et al. did not observe this signal for E. coli.[24] Differences to our methods include the reducing agent (boro-

hydride instead of hydroxylamine) as well as storing of the prepared bacterial cells at −80 °C prior to *in situ* AgNP synthesis. We observed the signal at 733 cm$^{-1}$ both with an excitation wavelength of 532 nm (3 s, 35 μW) and 633 nm (3 s, 138 μW) with similar spectral characteristics as presented by Premasiri *et al.* who used Au-nanoparticle-covered substrates and a 785 nm laser but log-phase cultures.[23] However, the signals at 733 cm$^{-1}$ and 668 cm$^{-1}$ were not observed for the other five microorganisms analysed in our work at the given measurement conditions. Premasiri *et al.* pointed out that the interaction time of metallic nanostructure and bacterial cells can play an important role for the occurrence of bacterial SERS signals and related this to the delayed enzymatic degradation and following secretion of metabolites (purines).[23] In our case intense SERS signals at 733 cm$^{-1}$ and 668 cm$^{-1}$ were observed for *E. coli* only, irrespective of the reaction time (up to 2 h). Other tested microbes were lacking this characteristic spectral information. Either these organisms do not release the molecules causing SERS signals at 733 cm$^{-1}$ and 668 cm$^{-1}$ to the same extent or other properties intervene with the applied preparation protocol. High variations between the single-cell spectra, which are included in Fig. S5/S6 of the ESI,† additionally limit the applicability of SERS to distinguish the microorganisms. Hence, the bands at 733 cm$^{-1}$ and 668 cm$^{-1}$ do not seem to be suited for all microorganisms, at least not with the excitation wavelength of 532 nm.

**Impact of culture storage onto SERS signals.** In the following we explored to what extent the appearance and intensity of microbial SERS signals is not only influenced by the identity of the investigated microorganism but also influenced by the physiological state of the cells. Fig. 2 displays fitted single-cell SERS intensities at 733 cm$^{-1}$ (not normalised) of freshly harvested *E. coli* cells that were cultured with LB medium to the stationary phase, and of cells from stationary phase cultures stored at 5 °C for 4 days prior to SERS analysis. After storage,

the averaged SERS intensity decreased significantly from 39 to 7 counts corresponding to a drop by over 80%. This sharp decline in signal intensity is also reflected in the number of actual SERS hits as listed in Table 1. The percentage of hits decreased significantly from 72% to 32% (*p*-value of 0.054 for unpaired heteroscedastic *t*-test). This finding is consistent with the above mentioned missing peak at 733 cm$^{-1}$ reported by Chisanga and coworkers[24] where the cells were stored at −80 °C before nanoparticle synthesis. In this context, also the large variance in signal intensity for single *E. coli* cells of freshly prepared cultures is worth to mention which likely reflect physiological variations among individual cells as typically found in stationary phase cultures. While 28% of the measured bacteria showed no signal, the SERS hits scattered from the cut-off value of 5 counts, up to the most intense signal of about 300 counts under precisely the same measurement parameters. The decrease in SERS intensity during storage of *E. coli* was also tested in minimal medium (Fig. 3a), where the declining signal and the scatter in number of hits is congruent with the results obtained with cells grown in the rich LB medium. It is also reflected in the steady decline of the maximal signal intensity recorded for increasing storage times. The strongest impact onto the percentage of SERS hits seems to occur already after one day of storage with a drop of 80% to 47%.

The decreasing SERS signal may be caused by two reasons: (1) the AgNP are not in close vicinity to microbial cells after sample preparation is finished. (2) The analyte(s) itself is(are) not present in the same condition or concentration. The first assumption was already considered for dead bacteria by Zhou *et al.* who reported that the signal at 735 cm$^{-1}$ decreased if *E. coli* cells were exposed to antibiotics as well as if varying percentages of autoclaved cells were added and explained this finding by a vanishing surface charge.[25] Indeed, also in the current study we did not observe any SERS signals for heat-killed *E. coli* cells when applying the same measurement parameters (data not shown). To test the hypothesis that the decrease in SERS signal could be attributable to the death of cells during storage we analysed the viability of *E. coli* by flow cytometry using the dyes propidium iodide (emission at 617 nm) and SYTO 9 (emission at 501 nm). These stains predominantly intercalate with nucleic acids of dead and living



**Fig. 2** Decreasing absolute SERS intensity at 733 cm$^{-1}$ of single *E. coli* (LB medium) cells which were cultured to the stationary phase and either directly subjected to *in situ* AgNP synthesis or first stored for 4 d. Values are scattered on the abscissa for better readability.

**Table 1** Percentage of actual SERS hits of *E. coli* cells cultivated with LB and M9 medium in biological triplicates at different storage times and following *in situ* AgNP synthesis

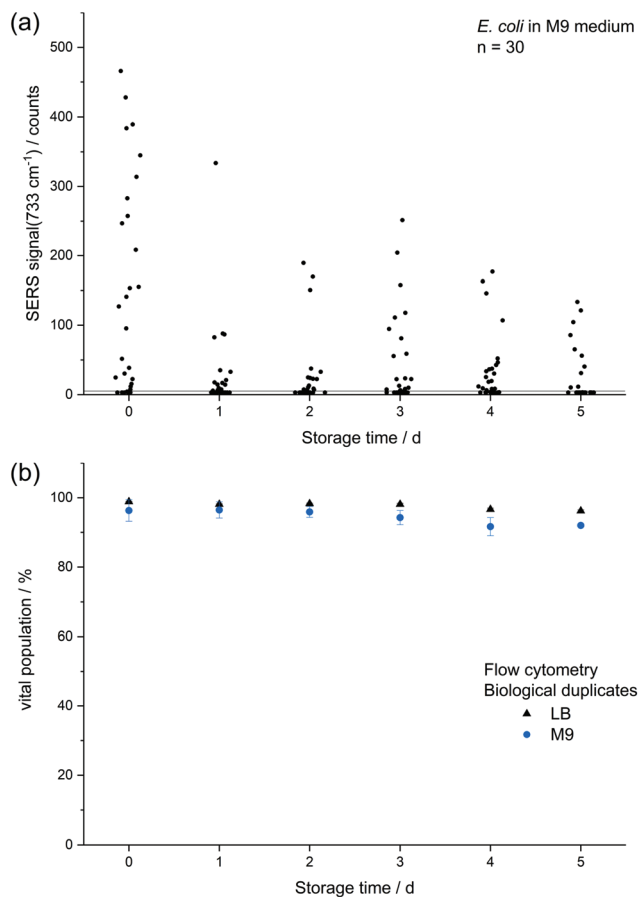| Storage time/d | Percentage of SERS hits ± 1 s/% LB medium | Percentage of SERS hits ± 1 s/% M9 medium |
|---|---|---|
| 0 | 72.2 ± 8.4 | 80.0 ± 10.0 |
| 1 | 46.7 ± 11.5 | 46.7 ± 23.1 |
| 2 | 30.0 ± 34.6 | 50.0 ± 10.0 |
| 3 | 40.0 ± 26.5 | 56.7 ± 35.1 |
| 4 | 50.0 ± 17.3 | 63.3 ± 15.3 |
| 5 | 32.2 ± 19.5 | 33.3 ± 20.8 |

(a)



(b)

**Fig. 3** Comparison of (a) absolute SERS signal at 733 cm$^{-1}$ of single *E. coli* cells which were cultured to the stationary phase and either directly subjected to *in situ* AgNP synthesis or first stored up to 5 d and (b) viability of *E. coli* measured by flow cytometry with two DNA intercalating dyes (propidium iodide: dead, SYTO 9: viable) after 0–5 d storage.

cells, respectively. Fig. 3b shows that the viability of the stored *E. coli* decreased only marginally by less than 5%. Therefore, flow cytometric analysis does not confirm the hypothesis that the decline in SERS signal is caused by dead bacteria. This result is in agreement with Colilert tests which revealed no noticeable drop of viability of the *E. coli* cells induced by the applied storage. We found more than 10$^9$ CFU ml$^{-1}$ in all the samples cultured in LB medium and 2 × 10$^8$ CFU ml$^{-1}$ in all of those in M9 medium (see Fig. S1b†).

Scanning electron microscopy (SEM) measurements were performed to investigate the hypothesis that missing AgNP were the reason for decreasing SERS signals. Fig. 4 illustrates that there is no significant difference for microbial samples which were either directly subjected to the *in situ* AgNP synthesis (a) or first stored for 12 d (b). Thus, we conclude that it must be the target analyte detected by SERS which disappears over storage time or can no longer be released by stored *E. coli* cells leading to the declining SERS signals. This finding was validated by mass spectrometric analysis of the metabolite adenine in the supernatant of washed *E. coli* cells. As shown in Fig. S7† the signal of adenine declines for samples of stored

cultures in comparison to freshly harvested, washed cells. Further, Chiu *et al.* recently report a rapid but over time decreasing release of purines by bacteria upon transferring them from a nutrient-rich into a nutrient-deprived environment.[42]

In bacteria approaching the stationary phase purine consumption by macromolecular synthesis abruptly slows.[43] Additionally, the cells start to break down free messenger ribonucleic acid (mRNA), transfer RNA (tRNA) and especially ribosomal RNA (rRNA).[44] This leads to a cellular accumulation of the end products of this degradation process including purine derivatives. The chemical nature of these products depends on the purine metabolic pathways present in the respective species, which vary considerably between bacterial species.[23] For *E. coli* the main end products will be adenine, xanthine, and hypoxanthine which are partially excreted. This accumulation and excretion happen within a time frame of about an hour after transferring the cells from medium into water or glucose deprived medium and is facilitated by the fact that hypoxanthine phosphoribosyl transferases operate close to the membrane and also transport their products through the membrane. The secretion of the purine derivatives might act as a signal for the culture to go into dormancy.[44] In addition to these phenomena, cyclic adenosine monophosphate is upregulated and also secreted in *E. coli* during glucose starvation and will thus contribute to the pool of extracellular purines in starved cultures. Furthermore, Bayer reported reversible cell wall disruptions upon hypoosmotic shock and the associated release of intracellular substances, *e.g.* acid-soluble nucleotides.[45] This starvation- and/or shock-induced breakdown and release of low-molecular weight nucleotides or degradation products well explains the characteristic *E. coli* SERS signal at 733 cm$^{-1}$. The phenomenon is able to relate our observations to a metabolic state instead of pure surface properties. Consequently, cells of microbial species like *E. coli* responding with these mechanisms to starvation or physiological stress (as induced by the cell washing procedure before nanoparticle synthesis) would be detectable by SERS if they are metabolically active to this point. Conversely, metabolically inactive and dormant cells would not release purine derivatives. Hence, they would show no or weak SERS signals even though they are viable, explaining the results obtained with stored *E. coli* cells. Furthermore, it is well known that several slow growing microorganisms (including nitrifiers such as *N. inopinata* and *N. gargensis*) show a much slower decrease in rRNA in response to starvation or stress[46–49] and might thus not exhibit the characteristic SERS signal at 733 cm$^{-1}$ even if they were metabolically active at the start of the cell washing and nanoparticle formation procedure.

## SERS of deuterated microbial cells

In addition to storage, also cultivation conditions seem to influence the results of the *E. coli* SERS analysis. Fig. 5a shows a comparison of *E. coli* cultured with M9 medium containing only normal water and with 25% (v/v) heavy water for 16 h, respectively. The red-shift up to 720 cm$^{-1}$ with a mean at

**Fig. 4** SEM images of *E. coli* cultured with M9 medium after 0 d (a) and 12 d (b) storage and following AgNP *in situ* synthesis.



**Fig. 5** (a) SERS signal at around 733 cm⁻¹ of *E. coli* with and without 25% D$_2$O addition plotted against Raman shift (bars: 1 s); (b) SERS intensity of *E. coli* with 25% addition of D$_2$O after 0 and 5 d storage. Note that the data at day 0 in the blue box of panel (b) corresponds to the deuterium data in the blue box of panel (a).

728 cm⁻¹ can be explained by the partial substitution of ¹H with D in the purine bases and their derivatives. The SERS intensity of the fitted peak at about 733 cm⁻¹ is significantly reduced for the deuterated cells. This effect is not expected to be related to a direct major impact onto the growth of *E. coli* as the growth curve of *E. coli* grown in media produced with concentrations of up to 25% of D$_2$O does not change fundamentally.[9,50] Surprisingly the position of the SERS purine bases band for deuterated cells varies stronger in comparison to unlabelled cells. The higher variance results either from varying amounts of incorporated deuterium into the purine bases, from changing positions of incorporated deuterium in purine bases or from a fundamental impact of heavy water onto the SERS causing mechanism, *e.g.*, the composition of released compounds. In any way, this indicates that conclusions onto the percentage of incorporated deuterium by certain microbial species based on this SERS peak is not as straight forward as for the stable isotopes ¹⁴N/¹⁵N.[4] The change of the SERS signal intensity of deuterated cells caused by storage over 5 d (Fig. 5b) is negligible in contrast to experiments with unlabelled *E. coli* cells (Fig. 3a). Thus, we suggest that either the formation or the release of the SERS target compound(s) is reduced because of incorporated deuterium.

The difference in SERS signal intensity and influence of storage on it between deuterated and unlabelled *E. coli* cells (Fig. 3a and 5b) underlines the impact of the physiological state of microbial target cells onto the results of SERS analyses and the necessity to conduct further research to explore how growth conditions and environmental factors affect microbial SERS signals in a species-dependent manner. On the other hand, our results suggest that SERS might be useful to analyse certain aspects of the physiology of *E. coli* with single-cell resolution, *e.g.* activity state of single cells or reaction upon stress conditions. Cells with distinct SERS signals likely are metabolic active.

The usefulness of spectroscopic techniques to detect active metabolic pathways or differentiate between certain physiological states was presented by Avetisyan *et al.* for Raman and by

Muhamadali *et al.* for infrared spectroscopy.[51,52] Stevenson *et al.* even demonstrated the detection of specific enzymatically catalysed reactions by SERS.[53] The applicability of SERS onto environmental samples was shown by Cui *et al.* who analysed the incorporation of stable isotope-labelled nitrogen sources with microcosms from surface water.[4] In the following sections we explore further opportunities for the applicability of SERS, in particular the strong signal at about 730 cm$^{-1}$ in *E. coli* cells, for SERS-assisted sorting by optical tweezers and SERS for 3D imaging at the single-cell level.

### Applicability of SERS for microbial detection

**SERS-assisted sorting by optical tweezing.** We applied the *in situ* SERS technique to sorting of *E. coli* cells by optical trapping. Fig. 6b shows the microscopic image with only the centre being in the laser focus. We were able to trap the bright particle showing the typical characteristics of *E. coli* SERS spectra at acquisition times as small as 100 ms. High laser powers nor-

mally lead to thermal degradation of dried SERS samples but can be increased in aqueous conditions. While the trapped particle showed high signals (Fig. 6a) the aqueous surrounding did not, indicating no detachment of AgNP with bound analyte (Fig. S8†). It should be noted that we deployed a centrifugation step following the AgNP *in situ* synthesis to remove excess reagent and avoid the formation of bubbles at strong laser irradiations. Additionally, this solved the problem of permanently occurring SERS signals which may be ascribed to the high cellular concentration. Upon dilution of the uncentrifuged sample, the signal was reduced but was still detectable without the trapping laser or microscopically visible cells in the focus (see Fig. S9†). A further possibility is the discussed release of molecules by microbial cells during *in situ* colloid synthesis. These molecules might diffuse into the sample fluid if not instantly and completely bound to formed AgNP on the surface of the *E. coli* cells themselves. Therefore, centrifugal separation was applied to minimise interference of aerogenic substances as well as potential evenly distributed SERS active compounds.

Experiments performed with a mixture of unlabelled and fully $^{13}$C-labelled *E. coli* proved that $^{13}$C-isotope incorporation into microbial cells can be measured by SERS of trapped cells (Fig. 6c). For two separate measurement events, we observed the normal SERS signal at 733 cm$^{-1}$ with unlabelled *E. coli* cells and the red-shifted signal at 720 cm$^{-1}$ for labelled cells. This detection of SERS signals of either fully labelled or unlabelled cells in a mixed sample combined with the optical evidence of separated cells suggest the applicability of SERS for sorting at the single-cell level. A general drawback of the experimental procedure is the necessity of an additional sample preparation step following *in situ* AgNP synthesis. The need for the removal of excess reagent implies difficulties to transfer the setup to more complex samples. The partial formation of larger aggregates because of the centrifugation calls for future optimization of the procedure. Especially the aforementioned discrepancy in SERS signals of different species represents a disadvantage for the use in sorting of unknown species.

### 3D SERS of microbial samples

The release of SERS-active metabolites implies also limitations for the use of SERS techniques for the spatially resolved imaging of microorganisms in environmental samples. Nevertheless, we tested the *in situ* AgNP synthesis as a way to accomplish also a three-dimensional detection of *E. coli*. Fig. 7 displays the 3D SERS image of a simplistic artificial biofilm model prepared with unlabelled and $^{13}$C-labelled *E. coli* cells which were washed before the *in situ* AgNP synthesis and afterwards mixed into the agarose gel.

Agarose gel is reported to be a suitable artificial model for biofilm research[54] and therefore was used in this study. The distinct signal at around 730 cm$^{-1}$ enables differentiation between labelled and unlabelled cells. The low integration time of 200 ms permits to scan volumes with grid intervals as depicted in Fig. 7 in about 30 min. Short measurements are



**Fig. 6** (a) Continuously acquired spectra of an AgNP@*E. coli* particle inside the laser focus. (b) Microscopic image during sorting by optical tweezing with an AgNP@*E. coli* particle inside the laser focus. (c) Consecutive SERS spectra of $^{13}$C-*E. coli* (red mean spectrum) and $^{12}$C-*E. coli* (blue mean spectrum) inside of the same sample with activated optical tweezer laser. Associated spectra are shifted on the ordinate for a better visualization.

**Fig. 7** 3D SERS image of $^{12}$C/$^{13}$C-labelled *E. coli* cells embedded into an agarose matrix. Not shifted and red-shifted SERS signal are drawn at each grid position in blue and red spheres respectively, the size and saturation represent the intensity. The corresponding rotating iso-surface plot is available in the ESI.†

required to precisely image aqueous biological samples as they are prone to misalign over time. Even though the SERS signal might be caused mainly by substances released from microbial cells we did not observe a broad dispersal of the SERS signal but found that it centred around cell structures. In addition, we tested the depth resolution of the Raman microspectroscopy setup with micrometre-sized synthetic polymer particles as shown in Fig. S10.† The results suggest that the depth resolution is sufficient to image micrometre-sized objects. Also, with a minimal ellipsoidal confocal volume of about 0.9 μm$^3$ the grid interval of one micrometre is adequate to scan for SERS signals of *E. coli* cells, which own similar dimensions.

## Conclusion

SERS spectra of six different microbial species (three Gram-negative, two Gram-positive and one archaeon) were analysed with identical measurement parameters giving rise to sharp peaks in case of *E. coli* but less distinct signals for the other species. The systematic comparison of fresh and stored *E. coli* cultures shows a rapid decrease of the SERS signal and the actual number of hits for single cells in stored cultures. This was the case both for bacteria cultured with a minimal medium as well as a full medium. The effect cannot be attributed to the death of cells since viability tests proved that after storage almost the same percentage of cells was still alive. SEM images showed that also in the case of stored cultures, *i.e.* cultures with lower SERS signal, AgNP were present on the cell surface eliminating detachment as another potential reason. We, therefore, relate the decline in SERS signal intensity to the metabolic activity of microbes and the release of nucleotides or their degradation products upon starvation and/or osmotic

shock, *e.g.*, adenine, guanine, hypoxanthine, xanthine as previously proposed.[23] SERS spectra of partially deuterated bacteria (<25%) exhibit a red-shift of the characteristic SERS band at 733 cm$^{-1}$ to 728 cm$^{-1}$, a surprisingly larger variance of the peak position and a stable intensity of the SERS signal in samples stored up to 5 days in contrast to non-deuterated samples. Again, our conclusion is that the SERS intensity represents the starvation-induced release of substances related to the metabolic activity. We conclude that it is mandatory to take into account, and to conduct further research on, the effect of the physiological state of microbes onto the SERS signal of microbial samples. Otherwise an incomplete understanding may give rise to pitfalls in the characterization and evaluation, and to misinterpretations. Further, we stress the implication of metabolites as a potential cause of SERS signals. Since released substances are not restricted to the immediate vicinity of cells but diffuse out, spatial attribution may be compromised. In our work, washing of microbial cells prior to the *in situ* AgNP synthesis eliminated possible SERS contributions of metabolites already released into the culture medium. This conclusion is confirmed by three-dimensional analyses, which did not show a uniform distribution of SERS signals, as would be expected for metabolites in aqueous solution. On the contrary, a biofilm model with $^{12}$C- and $^{13}$C-labelled *E. coli* gave a telling visualization that SERS events were strictly confined to cellular structures. The same holds true for the sorting of *E. coli* cells by optical trapping *via* SERS-based detection: upon an additional centrifugation step we were able to tweeze microbial cells and attached AgNP without the contribution of background SERS signals. We conclude that – despite the observed variability of SERS signals which warrants further investigation – SERS has a potential for detection, sorting, and characterization of metabolically active microorganisms at the single-cell level.

## Conflicts of interest

There are no conflicts to declare.

## Acknowledgements

microbial starvation and technical support from Markus Schmid.

# References

1 J. Xu, J. W. Turner, M. Idso, S. V. Biryukov, L. Rognstad, H. Gong, V. L. Trainer, M. L. Wells, M. S. Strom and Q. Yu, *Anal. Chem.*, 2013, **85**, 2630–2637.

2 S. Polisetti, A. N. Bible, J. L. Morrell-Falvey and P. W. Bohn, *Analyst*, 2016, **141**, 2175–2182.

3 H. Guo, B. Xing, L. C. Hamlet, A. Chica and L. He, *Sci. Total Environ.*, 2016, **554–555**, 246–252.

4 L. Cui, K. Yang, G. Zhou, W. E. Huang and Y. G. Zhu, *Anal. Chem.*, 2017, **89**, 5793–5800.

5 X. Lu, D. R. Samuelson, Y. Xu, H. Zhang, S. Wang, B. A. Rasco, J. Xu and M. E. Konkel, *Anal. Chem.*, 2013, **85**, 2320–2327.

6 A. K. Boardman, W. S. Wong, W. R. Premasiri, L. D. Ziegler, J. C. Lee, M. Miljkovic, C. M. Klapperich, A. Sharon and A. F. Sauer-Budge, *Anal. Chem.*, 2016, **88**, 8026–8035.

7 F. Chen, B. R. Flaherty, C. E. Cohen, D. S. Peterson and Y. Zhao, *Nanomedicine*, 2016, **12**, 1445–1451.

8 I. Marcaida, M. Maguregui, H. Morillas, C. Garcia-Florentino, V. Pintus, T. Aguayo, M. Campos-Vallette and J. M. Madariaga, *Anal. Bioanal. Chem.*, 2017, **409**, 2221–2228.

9 D. Berry, E. Mader, T. K. Lee, D. Woebken, Y. Wang, D. Zhu, M. Palatinszky, A. Schintlmeister, M. C. Schmid, B. T. Hanson, N. Shterzer, I. Mizrahi, I. Rauch, T. Decker, T. Bocklitz, J. Popp, C. M. Gibson, P. W. Fowler, W. E. Huang and M. Wagner, *Proc. Natl. Acad. Sci. U. S. A.*, 2015, **112**, E194–E203.

10 Y. Wang, W. E. Huang, L. Cui and M. Wagner, *Curr. Opin. Biotechnol.*, 2016, **41**, 34–42.

11 W. E. Huang, K. Stoecker, R. Griffiths, L. Newbold, H. Daims, A. S. Whiteley and M. Wagner, *Environ. Microbiol.*, 2007, **9**, 1878–1889.

12 E. Singer, M. Wagner and T. Woyke, *ISME J.*, 2017, **11**, 1949–1963.

13 C. Xie, D. Chen and Y.-Q. Li, *Opt. Lett.*, 2005, **30**, 1800–1802.

14 W. E. Huang, A. D. Ward and A. S. Whiteley, *Environ. Microbiol. Rep.*, 2009, **1**, 44–49.

15 Y. Wang, Y. Ji, E. S. Wharfe, R. S. Meadows, P. March, R. Goodacre, J. Xu and W. E. Huang, *Anal. Chem.*, 2013, **85**, 10697–10701.

16 E. C. Le Ru, P. G. Etchegoin and M. Meyer, *J. Chem. Phys.*, 2006, **125**, 204701.

17 S. Efrima and B. V. Bronk, *J. Phys. Chem. B*, 1998, **102**, 5947–5950.

18 R. M. Jarvis and R. Goodacre, *Anal. Chem.*, 2004, **76**, 40–47.

19 M. Kahraman, M. Müge Yazici, F. Şahİn, Ö. F. Bayrak, E. TopÇu and M. Çulha, *Int. J. Environ. Anal. Chem.*, 2007, **87**, 763–770.

20 P. Kubryk, J. S. Kolschbach, S. Marozava, T. Lueders, R. U. Meckenstock, R. Niessner and N. P. Ivleva, *Anal. Chem.*, 2015, **87**, 6622–6630.

21 L. Zeiri, B. V. Bronk, Y. Shabtai, J. Eichler and S. Efrima, *Appl. Spectrosc.*, 2004, **58**, 33–40.

22 P. Kubryk, R. Niessner and N. P. Ivleva, *Analyst*, 2016, **141**, 2874–2878.

23 W. R. Premasiri, J. C. Lee, A. Sauer-Budge, R. Theberge, C. E. Costello and L. D. Ziegler, *Anal. Bioanal. Chem.*, 2016, **408**, 4631–4647.

24 M. Chisanga, H. Muhamadali, R. Kimber and R. Goodacre, *Faraday Discuss.*, 2017, **205**, 331–343.

25 H. Zhou, D. Yang, N. P. Ivleva, N. E. Mircescu, S. Schubert, R. Niessner, A. Wieser and C. Haisch, *Anal. Chem.*, 2015, **87**, 6553–6561.

26 H. Daims, E. V. Lebedeva, P. Pjevac, P. Han, C. Herbold, M. Albertsen, N. Jehmlich, M. Palatinszky, J. Vierheilig, A. Bulaev, R. H. Kirkegaard, M. von Bergen, T. Rattei, B. Bendinger, P. H. Nielsen and M. Wagner, *Nature*, 2015, **528**, 504–509.

27 R. Hatzenpichler, E. V. Lebedeva, E. Spieck, K. Stoecker, A. Richter, H. Daims and M. Wagner, *Proc. Natl. Acad. Sci. U. S. A.*, 2008, **105**, 2134–2139.

28 M. Palatinszky, C. Herbold, N. Jehmlich, M. Pogoda, P. Han, M. von Bergen, I. Lagkouvardos, S. M. Karst, A. Galushko, H. Koch, D. Berry, H. Daims and M. Wagner, *Nature*, 2015, **524**, 105–108.

29 N. Leopold and B. Lendl, *J. Phys. Chem. B*, 2003, **107**, 5723–5727.

30 H. Zhou, D. Yang, N. P. Ivleva, N. E. Mircescu, R. Niessner and C. Haisch, *Anal. Chem.*, 2014, **86**, 1525–1533.

31 L. Cui, S. Chen and K. Zhang, *Spectrochim. Acta, Part A*, 2015, **137**, 1061–1066.

32 S. M. Beiser and B. D. Davis, *J. Bacteriol.*, 1957, **74**, 303–307.

33 S. Efrima and L. Zeiri, *J. Raman Spectrosc.*, 2009, **40**, 277–288.

34 R. M. Jarvis and R. Goodacre, *Chem. Soc. Rev.*, 2008, **37**, 931–936.

35 A. Walter, A. Marz, W. Schumacher, P. Rosch and J. Popp, *Lab Chip*, 2011, **11**, 1013–1021.

36 M. Kahraman, K. Keseroglu and M. Culha, *Appl. Spectrosc.*, 2011, **65**, 500–506.

37 A. Colnita, N. E. Dina, N. Leopold, D. C. Vodnar, D. Bogdan, S. A. Porav and L. David, *Nanomaterials*, 2017, **7**, 248.

38 H. Wetzel, B. Pettinger and U. Wenning, *Chem. Phys. Lett.*, 1980, **75**, 173–178.

39 R. M. Jarvis, A. Brooker and R. Goodacre, *Anal. Chem.*, 2004, **76**, 5198–5202.

40 Y. Liu, Y.-R. Chen, X. Nou and K. Chao, *Appl. Spectrosc.*, 2007, **61**, 824–831.

41 A. A. Guzelian, J. M. Sylvia, J. A. Janni, S. L. Clauson and K. M. Spencer, in *Vibrational Spectroscopy-Based Sensor Systems*, ed. S. D. Christesen and A. J. Sedlacek, SPIE—The International Society for Optical Engineering, Bellingham, 2002, vol. 4577, pp. 182–192.

42 S. W. Chiu, H. W. Cheng, Z. X. Chen, H. H. Wang, M. Y. Lai, J. K. Wang and Y. L. Wang, *Phys. Chem. Chem. Phys.*, 2018, **20**, 8032–8041.

43 Y. Kim, C. M. Lew and J. D. Gralla, *J. Bacteriol.*, 2006, **188**, 7457–7463.

44 U. Rinas, K. Hellmuth, R. Kang, A. Seeger and H. Schlieker, *Appl. Environ. Microbiol.*, 1995, **61**, 4147–4151.

45 M. E. Bayer, *J. Bacteriol.*, 1967, **93**, 1104–1112.

46 M. Wagner, G. Rath, R. Amann, H.-P. Koops and K.-H. Schleifer, *Syst. Appl. Microbiol.*, 1995, **18**, 251–264.

47 E. Morgenroth, A. Obermayer, E. Arnold, A. Brühl, M. Wagner and P. A. Wilderer, *Water Sci. Technol.*, 2000, **41**, 105–113.

48 A. Bollmann, I. Schmidt, A. M. Saunders and M. H. Nicolaisen, *Appl. Environ. Microbiol.*, 2005, **71**, 1276–1282.

49 E. French and A. Bollmann, *Life*, 2015, **5**, 1396–1404.

50 S. H. Kopf, S. E. McGlynn, A. Green-Saxena, Y. Guan, D. K. Newman and V. J. Orphan, *Environ. Microbiol.*, 2015, **17**, 2542–2556.

51 A. Avetisyan, J. B. Jensen and T. Huser, *Anal. Chem.*, 2013, **85**, 7264–7270.

52 H. Muhamadali, Y. Xu, D. I. Ellis, J. W. Allwood, N. J. Rattray, E. Correa, H. Alrabiah, J. R. Lloyd and R. Goodacre, *Appl. Environ. Microbiol.*, 2015, **81**, 3288–3298.

53 R. Stevenson, S. McAughtrie, L. Senior, R. J. Stokes, H. McGachy, L. Tetley, P. Nativo, J. M. Brewer, J. Alexander, K. Faulds and D. Graham, *Analyst*, 2013, **138**, 6331–6336.

54 M. Strathmann, T. Griebe and H. C. Flemming, *Appl. Microbiol. Biotechnol.*, 2000, **54**, 231–237.